

## Evaluation of Antioxidant Activity and Inhibition of Corrosion by Brazilian Plant Extracts and Constituents

José Milton Ferreira Júnior<sup>1,\*</sup>, Maria Goretti de Vasconcelos Silva<sup>1</sup>, Jackelyne Alve Monteiro<sup>1</sup>, Alexandre de Sousa Barros<sup>2</sup>, Maria Jose Cajazeiras Falcão<sup>2</sup> and Selene Maia de Morais<sup>2</sup>

<sup>1</sup> Departamento de Química Orgânica e Inorgânica, Universidade Federal do Ceará, 12200, CEP 60021-970 Fortaleza - CE, Brasil

<sup>2</sup> Curso de Química, Universidade Estadual do Ceará, Av. Dr. Silas Munguba 1700, CEP 60714-903, Fortaleza, CE, Brasil.

\*E-mail: [milton\\_ufc@yahoo.com.br](mailto:milton_ufc@yahoo.com.br)

Received: 20 January 2016 / Accepted: 23 February 2016 / Published: 1 April 2016

---

This study reports the ability of phenolic and amino compounds contained in extracts of plants from Northeastern Brazil of inhibiting corrosion and its correlation with antiradical activity. A phytochemical study of alkaloid extract leads to the isolation of a compound, whose structure was determined by nuclear magnetic resonance spectroscopy. The following were performed; the evaluation of antioxidant activity, electrochemical study by potentiodynamic linear polarization, electrochemical impedance spectroscopy, immersion tests and analysis by scanning electron microscopy. The chromatography techniques were used to isolate the amino compound, which was identified as 4-(N-methylamino)-benzoic acid by <sup>13</sup>C - and <sup>1</sup>H-NMR spectroscopy. This compound showed a superior anticorrosion performance than phenolic compounds and its origin extract. The adsorption phenomena had influence on corrosion inhibition more than antiradical activity.

---

**Keywords:** Carbon steel; Organic coatings; Acid corrosion; Adsorption, Antioxidant Activity.

### 1. INTRODUCTION

The problem of corrosion is common and occurs in various sectors, such as chemical industry, petrochemical, shipbuilding, construction, automotive, aviation, railway, maritime and others. The consequences of corrosion can result in economic loss, for example, the oxidation of residential pipes, vehicles and metal materials in general, but can also result in serious accidents, causing damage to both nature and man, for example, degradation in pipeline systems, bridge failures, and others[1,2].

The search for environmentally friendly corrosion inhibitors is certainly a current need, where the most common in industry are toxic. For example, ion chromium VI is an excellent inhibitor of iron

corrosion and its alloys, however, its irritating to mucous membranes and carcinogenic. Many organic compounds are known to be applicable as steel and copper corrosion inhibitors in acid environments. Usually, corrosion inhibitors are organic compounds that contain sulfur and oxygen nitrogen atoms linked to aromatic rings in a conjugated system, because these atoms or groups give the electronegative sites to the molecule to interact with the metal surface, through adsorption over the metal surface, forming a protective layer [3-6].

The aim of this work was to investigate the effects of etanolic extract in five plants from Northeastern Brazil as a corrosion inhibitor for carbon steel in HCl 0.1 M as natural corrosion inhibitors and its correlation with antiradical activity. For this the following were evaluated; the mass loss measure, electrochemical impedance spectroscopy (EIS), scanning electronic microscopy (SEM), and potentiodynamic linear polarization (PLP).

## 2. EXPERIMENTAL

### 2.1. Preparation of plant extracts:

The leaves of the species *Senna cana* (Nees & Mart.) HS Irwin & Barneby, *Byrsonima sericea* DC, *Dimorphandra gardneriana* Tul. and *Mangifera indica* L. and branches of *Zanthoxylum syncarpum* Tull. were collected in the state of Ceará, Brazil and plant extracts were obtained by maceration in aqueous ethanol (70:30) using 500 grams in each sample. The respective extracts were EESCL, EEBSL, EEDGL, EEMIL and EEZSB.

### 2.2. Phytochemical screening

Qualitative tests for secondary metabolites were performed based on Matos[7]. These tests were based on visual observation of the color change or precipitate formation after addition of specific reagents.

### 2.3. Determination of antioxidant activity

In the spectrophotometric procedure, 3.9 mL of a methanol solution of 2,2-Diphenyl-1-picrylhydrazyl (DPPH) at  $6.5 \times 10^{-5}$  M and 0.1 mL of methanol solutions of plant extracts (1000 ppm) or positive control (quercetin) were mixed and the absorbance of the reaction was read at 515 nm. The test was performed in triplicate at various concentrations of the plant extracts in mg/mL[8]. Absorbance measurements were determined in a Spekol 1100 spectrophotometer.

### 2.4. Quantification of total phenol content

Total phenolic content was determined by the spectrophotometric method using the Folin-Ciocalteu reagent, and gallic acid as reference standard[9]. Plant ethanol extracts (7.5 mg) were

dissolved in methanol and transferred to a 25 mL volumetric flask and final volume was completed with methanol. An aliquot of 100  $\mu\text{L}$  of the latter solution was shaken with 500  $\mu\text{L}$  of Folin-Ciocalteu reagent and 6 mL of distilled water for 1 min; after this time 2 mL of 15%  $\text{Na}_2\text{CO}_3$  were added to the mixture and stirred for 30s. Finally, the solution was settled to 10 mL volume with distilled water. After 2 h of incubation, the absorbance of the samples was measured at 750 nm.

### 2.5. Obtaining the alkaloid fraction

The extract EEZSB was subjected to acid-base extraction[9]. The results were interpreted using thin layer chromatography (TLC), with Dragendorff reagent for revealing.

After this, the alkaloid extract was subjected to column chromatography on silica gel with  $\text{Na}_2\text{CO}_3$  (5%) impregnated and using as eluents: hexane, chloroform, ethyl acetate and methanol in different proportions with increasing gradient of polarity [10]. The obtained fractions were submitted to TLC with mobile phase for specific alkaloids: ethyl acetate, ethyl methyl ketone, formic acid and water (50: 30: 10: 10)[9]. The fraction obtained in ethyl acetate and methanol (50:50) was purified by chromatography on Sephadex® column using ethyl acetate as the eluent and revealed with Dragendorff reagent. A compound was identified by  $^1\text{H}$  and  $^{13}\text{C}$  NMR spectroscopy.

After all of the described steps an ethanolic extract alkaloidal fraction of *Zanthoxylum syncarpum branches* (EEZSB - AF) was obtained.

### 2.6. Corrosion tests

The corrosion behavior was evaluated by potentiodynamic linear polarization (PLP) with a scan rate of  $1 \text{ mV}\cdot\text{s}^{-1}$ , potential scan between -1.5 and 0 V.

Electrochemical impedance spectroscopy was performed in open circuit with a sine wave of 10 mV amplitude at frequencies ranging from 100 kHz to 10 mHz. The impedance results are represented by Nyquist diagrams. All electrochemical measurements were obtained using potentiostat PGSTAT30 model (AUTOLAB, Metrohm - Eco Chemie).

The working electrode was a 1020 carbon steel disc inserted in epoxy resin with exposed area of about  $1 \text{ cm}^2$ . Platinum was used as an auxiliary electrode and the reference electrode (Ag/AgCl).

In the mass loss tests, the substrates (1020 carbon steel disc described above) were immersed in a solution of HCl 0.1 M in the absence and in the presence of extracts at a concentration of extract 20% at different times (30 minutes, 60 minutes, 240 minutes, 600 minutes and 1440 minutes.).

The corrosion rates for samples were obtained according to ASTM G1-90[11], whose calculation of corrosion rates in  $\text{mm}\cdot\text{year}^{-1}$ .

### 2.7. Morphologic characterization

The surface morphology of the electrodeposits was analyzed by a Philips XL-30 scanning electron microscope (SEM). The coating composition was analyzed by an energy dispersive X-ray (EDX) apparatus attached to the SEM.

### 3. RESULTS AND DISCUSSION

The phytochemical tests revealed that leaves and branches of *S. cana*, *M. indica*, *D. gardneriana* and *B. sericea* species presented a variety of secondary metabolites of the phenolic type, while the *Z. syncarpum* differently present alkaloids.

**Table 1.** Phytochemical screening of ethanolic extracts of plants.

Metabolite type	<i>S. cana</i> leaves	<i>Z.</i> <i>syncarpum</i> branches	<i>M.</i> <i>indica</i> leaves	<i>D. gardneriana</i> leaves	<i>B.</i> <i>sericea</i> leaves
Phenols	+	+	+	+	+
Alkaloids	-	+	-	-	-
Anthocyanidins	-	-	-	+	-
Anthraquinones	+	-	-	-	-
Steroids	+	+	-	-	-
Flavones	+	-	+	+	-
Flavonols	+	-	+	+	-
Saponins	-	-	+	+	+
Tannins	-	+	+	-	+
Triterpenoids	+	-	-	-	-
Xanthones	+	-	+	+	-

(+) Presence      (-) Absence

The results of the determination of total phenols, using Folin-Ciocalteu method, were expressed as gallic acid equivalents GAE/g of ethanol extract are presented on the Table 2.

**Table 2.** Total phenols and antioxidant activity.

Samples	Total Phenols	Antioxidant activity
	<sup>a</sup> mg EAG/g extract EtOH	<sup>b</sup> IC <sub>50</sub> (µg/mL)
EESCL	51.45 ± 0.95	10.06 ± 0.094
EEZSB	12.43 ± 0.62	140.29 ± 0.281
EEMIL	22.99 ± 0.29	26.23 ± 0.103
EEBSL	78.43 ± 1.64	49.74 ± 0.032
EEDGL	29.20 ± 0.30	71.79 ± 0.567
EEZSB - AF	-	56.17 ± 0.203
Quercetin (standard)	-	4.77 ± 0.050

<sup>a</sup>mg EAG/g extract: Concentration of phenols (mg) as gallic acid equivalent / gram of extract

<sup>b</sup>IC<sub>50</sub>: Minimum concentration capable of inhibiting 50% of the initial concentration of DPPH.

Samples that have a high content of phenolic substances, usually have good results for antioxidant activity[12], where this correlation can be more clearly seen in *S. cana* extract (EESCL),

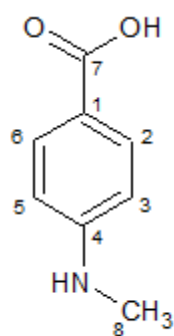
which obtained a relevant result of inhibition of DPPH radical. The antioxidant activity of phenolic compounds is mainly due to their reducing properties and chemical structure. These characteristics have an important role in the neutralization or sequestration of free radicals and the chelation of transition metals, acting both in the initiation and the propagation step of the oxidative process. The intermediates formed by the action of phenolic antioxidants are relatively stable due to the resonance of the aromatic ring in the structure of these substances [13,14]. The species *Z. syncarpum* (EEZSB) did not show significant amount of phenols, justifying its low antioxidant (high IC<sub>50</sub> value).

### 3.1. Structure elucidation of the isolated product from EEZSB - AF.

The <sup>1</sup>H and <sup>13</sup>C NMR spectra signals of isolated compound are shown in Table 3. The structure of 4-(methylamino)-benzoic acid was deduced by analysing the <sup>1</sup>H-NMR spectrum, which showed two doublets in aromatic region (7.74 and 6.86 ppm with J=8.43 Hz) suggesting the AA'BB' system, a singlet in 3.2 ppm characteristic of N-CH<sub>3</sub> and a singlet at 8.49 which could be a hydrogen from a carboxylic acid. In the <sup>13</sup>C-NMR spectrum, a carboxyl group was confirmed by the absorption at 169.89 ppm, the *para*-substituted system was confirmed by two more intense peaks at 131.18 (2C) and 116.92 and the N-CH<sub>3</sub> with a peak at 29.60 ppm [15]. The complete assignment of peaks was shown in table 3. Amides, alkaloid and coumarins have been isolated from this specie [16, 17], but the has no record in the literature for 4-(methylamino) benzoic acid as a natural product.

**Table 3.** <sup>1</sup>H and <sup>13</sup>C NMR assignments of the alkaloid from EEZSB – AF

Carbons	$\delta^{13}\text{C}$	$\delta^1\text{H}$
C <sub>1</sub>	127.42	-
C <sub>2</sub> , C <sub>6</sub>	131.18	7.12(d, J=8.43 Hz)
C <sub>3</sub> , C <sub>5</sub>	116.92	6.77(d, J=8.43 Hz)
C <sub>4</sub>	157.96	-
C <sub>7</sub>	169.89	8.49(s)
C <sub>8</sub>	29.60	3.20(s)



4-(methylamino)benzoic acid

**Figure 1.** Representation of the molecular structure of the amino compound found in EEZSB - AF

3.2. Electrochemical experiments

3.2.1. Potentiodynamic Linear Polarization (PLP)

The effect of the ethanolic extracts of the species tested were evaluated from the polarization curves obtained by PLP, represented in Figure 2, wherein a change in corrosion potential to more positive values can be seen. It is clear from Figure 2 that Tafel slope of the anodic ( $\beta_a$ ) and cathodic ( $\beta_c$ ) are significantly decreased in the presence of evaluated extracts, characterizing a adsorption of the inhibitor molecules[18]. These results indicate all extracts act as mixed type inhibitors (or adsorption inhibitors), which they act as protective films forming the cathode regions by inhibiting the reduction of oxygen and anodic minimizing the oxidation of the steel. Some silicates and phosphates which in neutral media with low chloride content and in the presence of oxygen, cause passivation of the steel (anodic inhibitor) and precipitate the cathode regions (cathode inhibitors) and organic film formers compounds (adsorption inhibitor) with two functional groups or mixture of compounds, some inhibitors acting as anode, cathode and the other acting as protective films [18, 19].

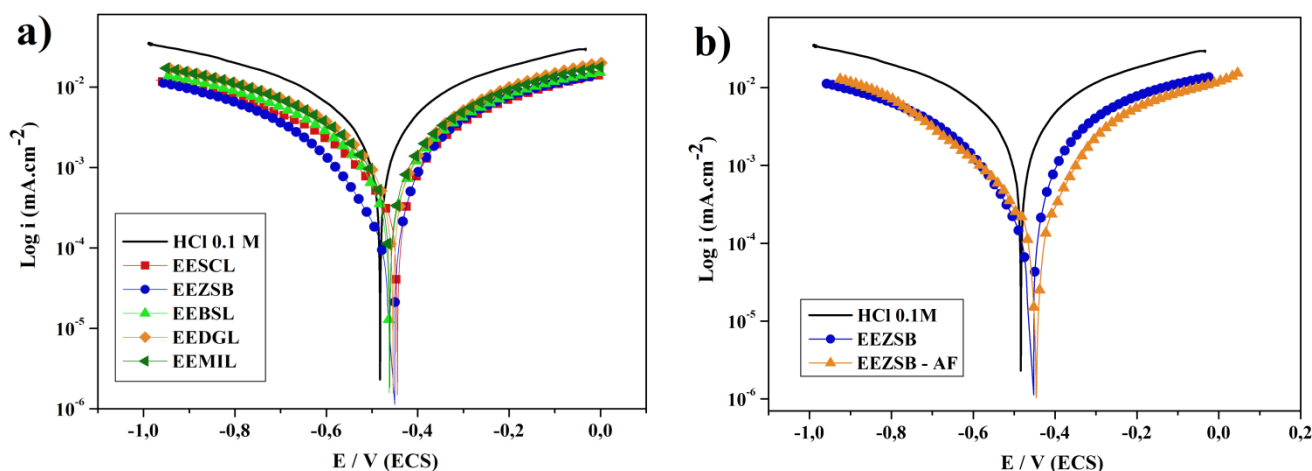


**Figure 2.** Polarization potentiodynamic curves for carbon steel immersed in HCl 0.1 M a) Crude extract to all species. b) EEZS(crude extract) vs. EEZS - AF.

From the Tafel slopes in the PLP, the polarization resistance ( $R_p$ ) can be obtained using the Stern – Geary equation (Eq. 1) [20], where this resistance value is inversely proportional to the corrosion current, therefore, related to the speed of corrosion process, therefore, an important parameter to be analyzed.

$$I_{corr} = \left[ \frac{\beta_a \times \beta_c}{2,303(\beta_a + \beta_c)} \right] \times \frac{1}{R_p} \tag{1}$$

Where  $\beta_a$  and  $\beta_c$  are respectively the anodic and cathodic Tafel slopes.  $I_{corr}$  is corrosion rate or corrosion current density in  $\text{mA.cm}^{-2}$ .

The  $R_p$  values (table 4), show that EEZSB-AF has the highest value of this variable ( $34.91 \text{ } \Omega.\text{cm}^{-2}$ ). As the polarization resistance is inversely proportional to the corrosion current, this inhibitor has a lower corrosion kinetics compared with other inhibitors investigated [20].According to

literature[3, 19, 21], this superiority of amino compounds may be related to the presence of organic compounds with O, N and S in its structure.

For calculating inhibition efficiency from PLP, the following formula was used:

$$\eta(\%) = \frac{I_0 - I_{inh}}{I_0} \times 100 \quad (2)$$

where  $I_0$  is the corrosion current density in the absence of an inhibitor and  $I_{inh}$  is the corrosion current density in the presence of an inhibitor. The corrosion current density ( $I$ ) is determined from the intercept of extrapolated cathodic and anodic Tafel slopes.

**Table 4.** Corrosion rates and electrochemical parameters derived from PLP.

Working Solution	$I_{corr}$ (mA.cm <sup>-2</sup> )	$E_{corr}$ (V/SCE)	$\beta_a$ (V.dec <sup>-1</sup> )	$\beta_c$ (V.dec <sup>-1</sup> )	$R_p$ (Ω.cm <sup>-2</sup> )	$\eta\%$
HCl 0.1 M	0,00255	-0.482	0.129	0.136	11.24	-
EESCL	0,00073	-0.449	0.101	0.099	29.47	71.37
EEZSB	0,00056	-0.444	0.090	0.084	32.97	78.03
EEZSB-AF	0,00051	-0.439	0.086	0.081	34.91	80.01
EEBSL	0,00083	-0.462	0.111	0.108	28.13	67.45
EEDGL	0,00095	-0.453	0.113	0.110	25.35	62.74
EEMIL	0,00098	-0.461	0.116	0.112	24.84	61.56

### 3.2.2. Weight Loss

The inhibition efficiencies (table 4) for weight loss tests were evaluated using the following formula:

$$\eta(\%) = \frac{W - W_i}{W} \times 100 \quad (3)$$

where  $W$  is the weight loss in the absence of an inhibitor and  $W_i$  is the weight loss in the presence of an inhibitor.

**Table 5.** parameters obtained from the mass loss tests

Working Solution	$\Sigma$ Mass (g)	$V_{corr}$ (mm.y <sup>-1</sup> )	$\eta\%$
HCl 0.1 M	0.0214g ± 0.0011	5.37 ± 0.117	-
EESCL	0.0058g ± 0.0004	1.06 ± 0.075	72.89
EEZSB	0.0041g ± 0.0004	0.76 ± 0.074	80.84
EEZSB-AF	0.0038g ± 0.0003	0.65 ± 0.043	82.24
EEBSL	0.0061g ± 0.0003	1.12 ± 0.069	71.49
EEDGL	0.0052g ± 0.0005	0.95 ± 0.085	75.70
EEMIL	0.0092g ± 0.0003	1.69 ± 0.055	57.01

The corrosion rate ( $V_{corr}$ ) on millimeters per year for carbon steel samples (table 4) were obtained according to ASTM G1-90[11], when the mass loss is known can be given by the following equation:

$$V_{corr} = \frac{3,65 \times \Delta m}{S \times t \times \rho} \tag{4}$$

whose  $\Delta m$  is Loss of weight, in mg;  $S$  is exposed area in  $\text{cm}^2$ ;  $t$  is exposure time in days and  $\rho$  is Specific mass of the material in  $\text{g.cm}^{-3}$ .

The mass loss (Figure 3) confirms that compounds rich in alkaloids exhibited higher efficiency. This characteristic is justified by the presence of aromatic rings and heteroatoms with conjugated double bonds present in isolated alkaloid (4-methylamino) benzoic acid [21-24]. These results show superior efficiency compared with inorganic inhibitors, such as sulfate N-methyl-p-aminophenol (metol), which have maximum inhibition efficiency of 81.9% to 27.5  $\text{g.dm}^{-3}$  (27000 ppm) [22]. However, the concentrations used in this study (1000 ppm) were much lower than the inorganic inhibitor, this associated toxicity of these compounds [22-24] shows importance based corrosion inhibitors natural products.

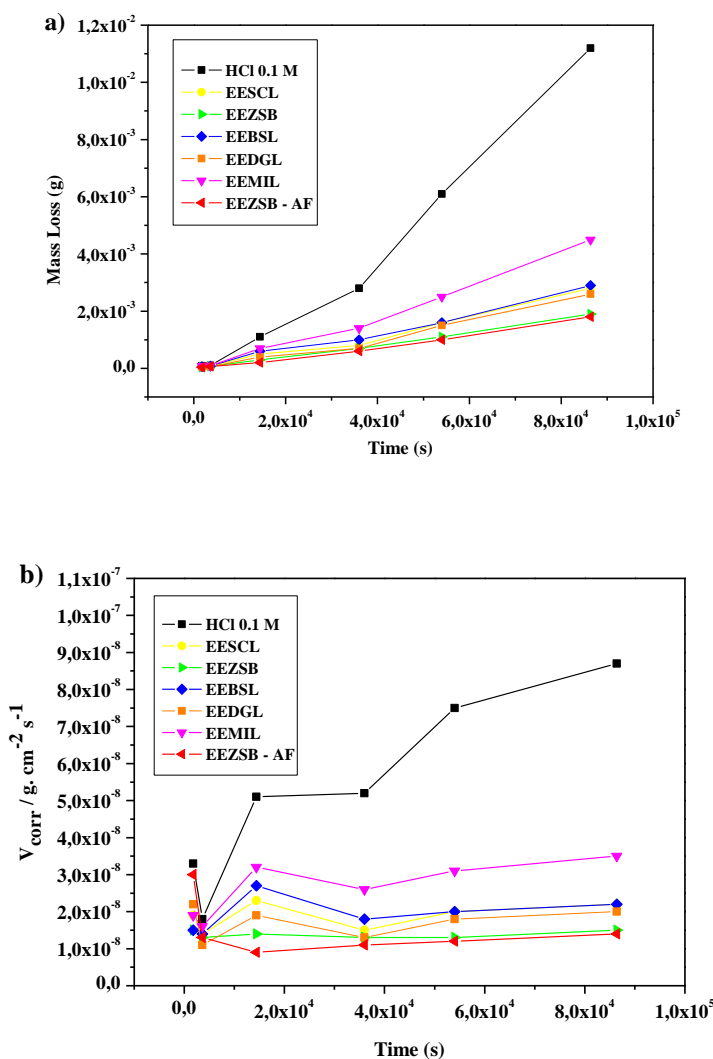


**Figure 3.** Mass loss tests (a) and corrosion rate (b) for phenolic and amino compounds.



3.2.3. Electrochemical Impedance Spectroscopy (EIS)

The Nyquist diagram, obtained by EIS (Figure 4), compares the efficiency in inhibiting corrosion of samples, wherein resistance to current passage of each sample is represented by a curve where the increase in slope of this curve indicates an increase in resistance charge transfer at the electrode / solution interface and results in a decrease in the tendency to corrode.

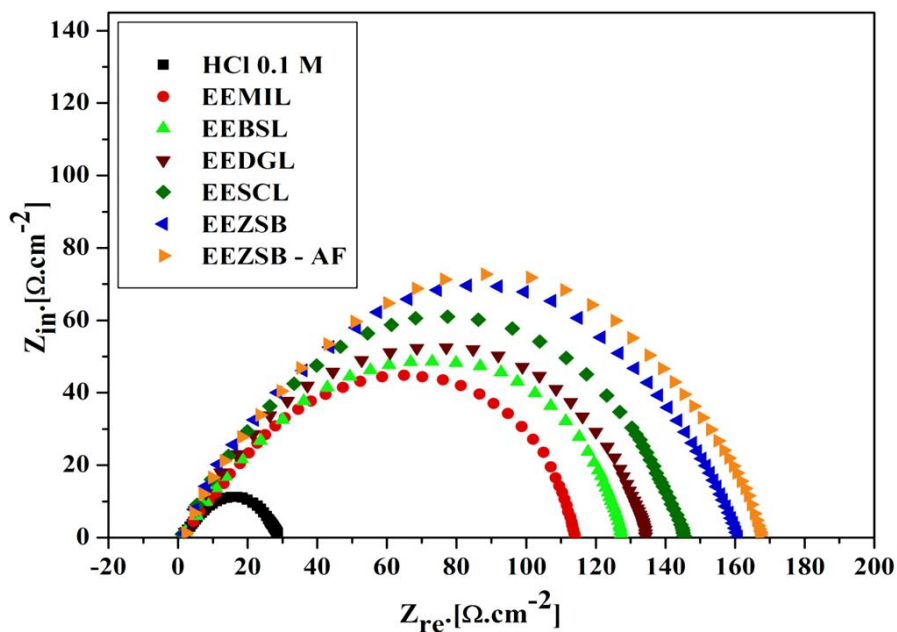


Figure 4. Nyquist diagram for phenolic and amino species.

From the Nyquist diagram (Figure 4), there is a significant increase in resistance for all species in comparison to the solution without extract (blank), so that the increased capacitive arc occurs more efficiently in amino compounds, particularly EEZSB - AF, emphasizing the relevant corrosion inhibiting ability of this species.

Table 5, show the parameters obtained from EIS, wherein the charge transfer resistance ( $R_{ct}$ ) was obtained by the difference between the impedances at lower and higher frequencies, the real axis intercept ( $Z_{in} = 0$ )

The double layer capacitance ( $C_{dl}$ ) is calculated using equation 05[25, 26]:

$$C_{dl} = 1/2\pi f_{max} R_{ct} \tag{5}$$

Where  $f_{max}$  is the frequency value at which the imaginary component of the impedance is maximum.

The fraction of the surface that was covered by adsorbed molecules was calculated according to equation 06[25]:

$$\theta = (1 - C_{dl}/C_{dl}^0) \tag{6}$$

Where  $C_{dl}$  and  $C_{dl}^0$  is the capacitance of the double layer determined with and without the presence of the extract in the solution, respectively.

The inhibition efficiency ( $\eta_{inh}\%$ ), was calculated using Eq. 7:

$$\eta(\%) = \frac{R_{ct(inh)} - R_{ct}}{R_{ct(inh)}} \times 100 \tag{7}$$

where  $R_{ct}$  and  $R_{ct(inh)}$  are referred to as the charge transfer resistance without and with the addition of the inhibitor, respectively.

**Table 6.** Impedance data and grade of coverage ( $\theta$ ) of carbon steel surface in 1020 in HCl 0.1 M and solutions containing plant extracts.

Samples	$R_{ct}$ ( $\Omega.cm^2$ )	$C_{dl}$ ( $\mu F.cm^{-2}$ )	$\eta\%$	$\theta$
HCl 0.1 M	26.55	90.28	-	-
EEMIL	112.02	17.20	76.30	0.81
EEBSL	125.38	19.12	78.82	0.79
EEDGL	132.28	14.57	79.92	0.83
EESCL	144.17	16.63	81.58	0.81
EEZSB	159.12	12.11	83.31	0.86
EEZSB-AF	167.21	11.52	84.12	0.87

The data presented in Table 5 shows a behavior similar to that observed in Tafel slopes and mass loss. From the values obtained from  $R_{ct}$  and  $C_{dl}$ , it is observed that the plant extracts decrease the capacitance of the double layer and increases the resistance to charge transfer, since there is an increased diameter of the semi-circle observed in the Nyquist diagrams. The adsorption may be responsible for lower capacitance in the presence of the inhibitor. The double layer formed at the electrode - solution interface is considered an electrical capacitor, where a decrease in capacitance is due to the formation of a protective barrier for organic molecules on the surface of the steel, which reduces the area available for reaction to occur in the carbon steel surface [27].

### 3.2.4. Adsorption Isotherm

To evaluate the adsorption process to extract that showed the best efficiency in inhibiting corrosion (EEZSB - AF), the adsorption isotherms of Langmuir and Temkin were obtained, from the coverage fraction ( $\theta$ ), calculated for different concentrations of EEZSB - AF presented in Table 6.

**Table 7.** Electrochemical parameters and grade of coverage for different concentrations of EEZSB - AF on HCl 0.1 M.

	Concentration ( $g.L^{-1}$ )	$R_{ct}$ ( $\Omega.cm^2$ )	$C_{dl}$ ( $\mu F.cm^{-2}$ )	$\theta$
HCl 0.1 M	3.65	26.55	90.28	--
EEZSB - AF	1.0	167.21	11.52	0.87
	0.4	129.53	15.77	0.82
	0.2	107.27	20.02	0.78
	0.1	93.41	25.66	0.71

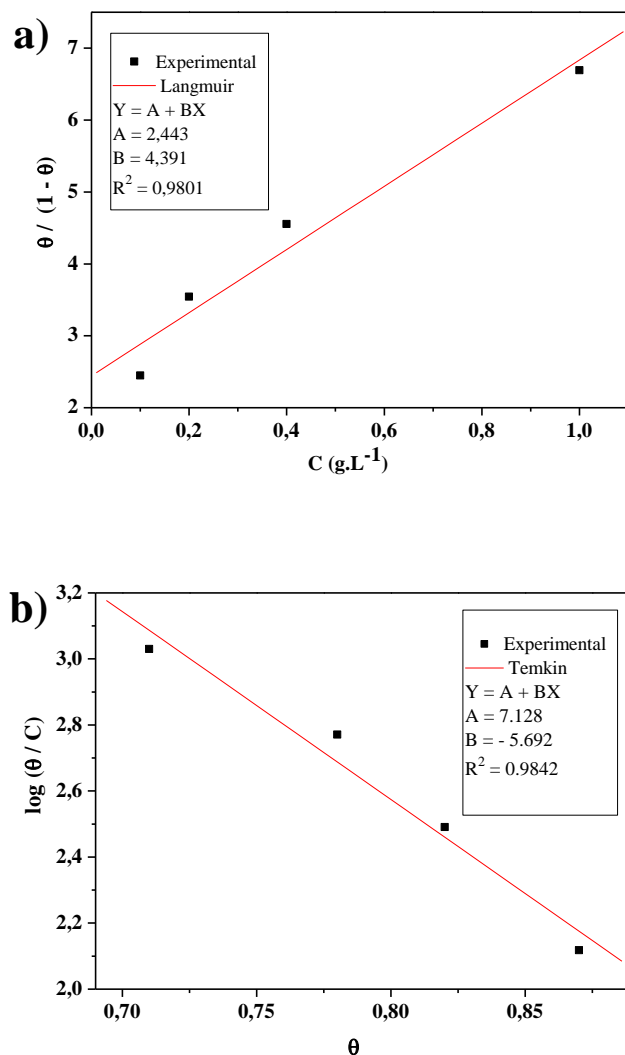


**Figure 5.** Langmuir adsorption isotherm (a) and Temkin adsorption isotherm (b) for carbon steel in HCl 0.1 M in different concentrations EEZSB - AF.

With the data obtained in the electrochemical impedance tests (Table 6) for the concentrations studied, it was possible to determine the grade of the coverage, making it possible to evaluate the Langmuir adsorption isotherm (Figure 5a).

The adsorption free energy for EEZSB-AF was calculated from the data obtained from the Langmuir adsorption isotherms, applied to the equation 08:

$$K_{ads} = \frac{1}{55,5} \exp - \left( \frac{\Delta G^\circ}{RT} \right) \tag{8}$$

Where 55.5 is the concentration of water in the solution in mol L<sup>-1</sup>, R is the gas constant (8.3147 J.mol<sup>-1</sup>.K<sup>-1</sup>), T is the temperature in K and ΔG° it is the standard free energy adsorption.

Therefore, a value for ΔG<sub>ads</sub> = -20.78 kJ.mol<sup>-1</sup> was obtained. However, the module of the values for ΔG° are less than 25 kJ.mol<sup>-1</sup>, concluding that the adsorption is purely physical [28, 29].

This parameter is a relevant factor for the evaluation of the substance efficiency that acts as an inhibitor. When the anions present in solution, such as chloride ions are adsorbed on the metal surface, there is the increased adsorption of organic cations on them, and then this is the way the inhibitor can be adsorbed on the metal surface [28- 30].

For the lateral grade of interaction, which was obtained from analysis of the results adjusted to Temkin adsorption isotherms (Figure 5b) showed  $g = - 5.692$ . The negative value indicates that the lateral interaction between the adsorbate molecules on the metal surface is repulsive [29, 30].

### 3.2.5. Morphological investigation

Figure 7A shows the scanning electron microscopy (SEM) images, obtained for polished 1020 carbon steel (magnification  $\times 1,000$ ), where a rough surface was observed, characteristic of uniform corrosion of carbon steel in acid medium, with the presence also of cracks and dendrites. In figure 07B a smooth surface can be observed, indicating that the surface was covered by the inhibitor. These results confirm the electrochemical analysis, showing that the substances in the ethanol of *Z. syncarpum* extract feature favors adsorption film formation [31,32].

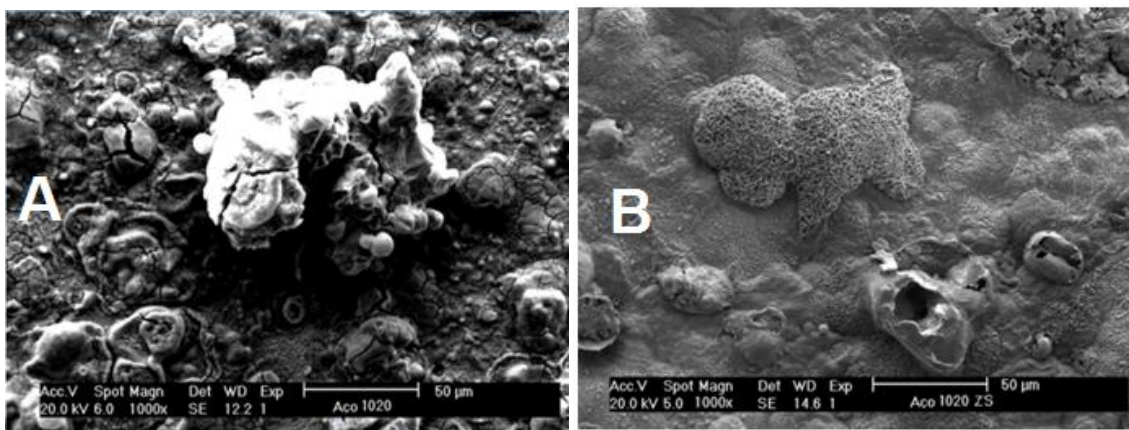


**Figure 6.** SEM images obtained for 1020 carbon steel after 240 minutes immersion in HCl 0.1 M in the absence (A) and presence (B) of *Z. syncarpum* EtOH extract at 1000 ppm.

## 4. CONCLUSION

The phytochemical tests revealed that EESCL, EEMIL, EEDGL and EEBSL species present as main secondary metabolites phenolic compounds, while *Z. syncarpum* also has alkaloids or amino-compounds. The anti-radical activity is not directly related to the inhibition of corrosion, indicating that the mechanism may be associated with adsorptive surface processes. The electrochemical analysis showed that extracts containing amino compounds displayed superior corrosion inhibiting properties than extracts without this. These results also show superior efficiency compared with inorganic inhibitors, such as sulfate N-methyl-p-aminophenol (Metol), offering superior efficiency, operating satisfactorily at much lower concentrations. With the determination of free energy of adsorption ( $\Delta G_{ads}$

= -20.78 kJ mol<sup>-1</sup>) calculated from the Langmuir isotherm, it can be concluded that the adsorption is purely physical.

The grade of lateral interaction, obtained from the Temkin adsorption isotherms showed a value of  $g = -5.692$ . The negative value indicates that the lateral interaction between the adsorbed molecules on the metal surface is repulsive.

The isolated compound (4-methylamino) benzoic acid showed the best results, suggesting that efficient inhibition of *Z. syncarpum* extract could be due to its presence.

## REFERENCES

1. B. E. A. Rani, B. B. J. Baju, *Int. j. corros.* 20 (2012) 1 - 15.
2. O. Benali, H. Benmehdi, O. Hasnaoui, C. Selles, R. Salghi, *J. Mater. Environ. Sci.* 4 (2013) 127.
3. T. H. Ibrahim, Z. A. Mohamed, *Int. J. Electrochem. Sci.* 6 (2011) 6442 - 6455.
4. P. C. Okafor, V. I. Osabor, E. E. Ebenso, *Pigm. Resin Technol.* 36 (2007) 299 - 305.
5. M. A. Quraishi, A. Singh, V. K. Singh, D. K. Yadav, A. K. Singh, *Mater. Chem. Phys.* 122 (2010) 114 - 122.
6. M. A. Chidiebere, C. E. Ogukwe, K. L. Oguzie, C N. Eneh, E. E. Oguzie, *Ind. Eng. Chem. Res.* 51 (2012) 668 - 677.
7. F. J. A. Matos, *Introdução à fitoquímica Experimental*, UFC, Fortaleza (2009).
8. J. G. A. Silva, J. A. Monteiro, E. B. Ferreira, C. G. Sampaio, M. V. G. Silva, *Int. J. Pharm. Pharm.* 6 (2014) 199 - 202.
9. H. Wagner, S. Bladt, *Springer-Verlag.* (1996).
10. A. A. Silva, S. M. Morais, M. J. C. Falcão, I. G. Vieira, L. M. Ribeiro, S. M. Viana, M. J. Teixeira, F. S. Barreto, R. Cardoso, H. F. Andrade-Júnior. *Phytomedicine.* 21 (2014) 1419 - 1423.
11. ASTM, G 1-90, *American Society for Testing and Materials*, 1998 Annual Book of ASTM Standards, Philadelphia (1999).
12. K. H. Lin, H. Y. Lin, C. M. Yang, H. J. Tsai, P. Y. Chao, *J. Food. Nutr. Res.* 2 (2014) 435 - 442.
13. F. Cuyckens, M. Claeys, *J. Mass Spectrom.* 39 (2004) 1 - 15.
14. J. M. Almeida, M. I. Genovese, F. M. Lajolo, *Ciênc. Tecnol. Aliment.* 26 (2006) 446 - 452.
15. D. Banfi, L. Patiny, *Chimia*, 62 (2008) 280 - 281.
16. S. A. Ross, G. N. Sultana, C. L. Burandt, M. A. Elsohly, P. J. Marais, D. Ferreira, *Nat. Prod.* 67 (2004) 88 - 90.
17. S. A. Ross, M. A. Al-Azeib, K. Krishnaveni, C. L. Burandt, *J. Nat. Prod.* 68 (2005) 1297 - 1299.
18. N. S. Patel, S. Jauhariandi, G. N. Mehta, S. S. Al-Deyab, I. Warad, B. Hammouti, *Int. J. Electrochem. Sci.* 8 (2013) 2635 - 2655.
19. P. Lima-Neto, A. N. Correia, G. P. Silva, *p. J. Bras. Chem. Soc.* 17 (2006) 1419 - 1427.
20. M. Curioni, F. Scenini, T. Monetta, F. Bellucci. *Electrochim Acta.* 166 (2015) 372 - 384.
21. D. A. R. Abdullah, *Ind. Lubr. Tribol.* 63 (2011) 227 - 233.
22. B. M. Praveen, T. V. Venkatesha, *Int. J. Electrochem. Sci.* 4 (2009) 267 - 275.
23. M. A. Maciel, C. C. Almeida, M. B. M. Cansanção, L. S. A. Moura, M. L. Medeiros, S. R. B. Medeiros, D. R. Silva, *Nanobiotechnology.* 11 (2014) 95 - 112.
24. M. H. Hussin, M. J. Kassim, *J. Phys. Sc.* 21 (2010) 1 - 13.
25. M. A. Deyab, S. S. Abd El-Rehim, *Int. J. Electrochem. Sci.* 8 (2013) 12613 - 12627.
26. C. G. M. Oliveira, V. W. Faria, G. F. Andrade, E. D'Elia, M. F. Cabral, B. A. Cotrim, G. O. Resende, F. C. de Souza, *Phosphorus Sulfur Silicon Relat Elem.* 190 (2015) 1366 - 1377.
27. D. E. Abd El-Khalek, B. Abd El-Nabeyb, A. Abd El-Gaberb, *Electr. Acta.* 30 (2012) 347 - 359.
28. L. Bammou, R. Salghi, A. Zarrouk, H. Zarrok, S. S. Al-Deyab, B. Hammouti, M. Zougagh, *Int.*

*J. Electrochem. Sci.* 7 (2012) 8974 - 8987.

29. S. Jyothi, J. Ravichandran, *Acta Metall. Sin.* 27 (2014) 969 - 980.
30. E. A. Noor, A. H. Al-Moubaraki, *Mater. Chem. Phys.* 110 (2008) 145 - 154.
31. M. A. Ameer, A. M. Fekry, *Prog. Org. Coat.* 71 (2011) 343 - 349.
32. S. Yahya, N. K. Othman, A. R. Daud, A. Jalar, *Sains Malays.* 47 (2014) 1083 - 1087.

© 2016 The Authors. Published by ESG ([www.electrochemsci.org](http://www.electrochemsci.org)). This article is an open access article distributed under the terms and conditions of the Creative Commons Attribution license (<http://creativecommons.org/licenses/by/4.0/>).